Journal of Thermal Analysis, Vol. 42 (1994) 467-484

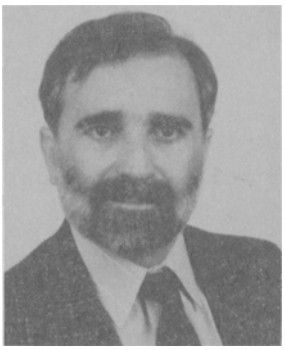

DUAL-MECHANISM KINETICS OF POLYPHENYLENE SULFIDE (PPS) MELT-CRYSTALLIZATION

J. A. Ferrara[1] *J. C. Seferis*[*1], *and C. H. Sheppard*[2]

[1]Polymeric Composites Laboratory Department of Chemical Engineering, University of Washington, Seattle, Washington 98195
[2]Boeing Defense and Space Systems, P.O. Box 3999 - MS 73–09 Seattle, Washington 98124, USA

Abstract

This investigation demonstrates that polyphenylene sulfide (PPS) crystallizes in a unique dual-mechanistic fashion in which 8% of the material by volume crystallizes instantaneously, while the remaining material crystallizes in a time dependent fashion. These rapid melt-crystallization kinetics are quantitatively modeled using a dual-mechanistic model approach which is based on the methodology first observed by Velisaris and Seferis in polyetheretherketone (PEEK) crystallization. The crystallization model is then used to accurately predict both isothermal and for the first time non-isothermal crystallization behavior over a wide spectrum of cooling rates utilizing the same model parameters. Specifically, this work identifies and models the initial fast crystallization kinetics of PPS. Additionally, the versatility of the Velisaris and Seferis dual-mechanistic model has been established with PPS, by simply showing that it is a special case of the generalized dual-crystallization kinetics methodology.

Keywords: crystallization kinetics, dual-mechanism, PPS, PEEK

Introduction

Polyphenylene sulfide (PPS) is a popular semi-crystalline engineering thermoplastic used in a variety of applications. Because of its versatility and relatively simple chemical structure, the fundamental physicist and the practitioner

* Author to whom correspodence should be addressed.

0368–4466/94/ $ 4.00

John Wiley & Sons, Limited
Chichester

alike have been able to make significant inroads into the fundamental and practical understanding of this material Although the purpose of this paper is to focus on a practical application of kinetics modeling, it is first necessary to point out that without the fundamental work of molecular physicists and chemists, such as Wunderlich, Lovinger, etc., the engineering practitioner would not have the benefit of a scientific basis in which to solve problems that arise on the engineering floor [1–3]. Thus, in order to avoid meaningless data plotting and allow for substantive extrapolation of behavior, robust engineering models must be developed that simultaneously provide the convenience and usefulness of simple descriptions of data with scientific legitimacy and bounds. It is in this light that this investigation produces a practical and useful engineering model for PPS crystallization.

Although PPS was first reported in 1897, a commercially successful synthesis was not developed until 1967 [4–6]. Early investigations focused on the crystalline structure, where as more traditional engineering properties were not examined until 1976 [4, 7–9]. Since then, PPS has been a very intensely studied material. It has a relatively simple chemical structure that is found commonly in the literature, good mechanical and chemical properties and excellent processing characteristics, all of which result in it being used in a variety of engineering applications, from injection molded products to matrices in high-performance composites [1, 3, 9–11]. Coupled with a glass transition temperature (T_g) of of 85–90°C and a melt temperature (T_m) of 280–285°C, these physical characteristics have made this material a prime candidate for detailed theoretical and practical study.

Because PPS is a semi-crystalline thermoplastic, it is typically processed by first melting the material and then processing it through various techniques, such as injection molding and blow-molding. During processing, the material cools and crystalline regions form as the material solidifies. Since the microstructure of semi-crystalline polymers ultimately determines the physical properties of the material, the amount and type of crystallinity that forms is important to know in order to predict end use properties such as moduli, toughness, *etc.* [12–16]. Thus, many investigations have focused on the crystallization behavior of PPS [3, 17–24]. Additionally, crystallization phenomena, in competition with thermal expansion effects, have been shown to promote matrix microcracking during the processing of composites [25]. Since PPS has been shown to be sensitive to microcracking, the importance of understanding the crystallization kinetics becomes paramount [26–27].

A significant overview of PPS investigations was offered by Lopez and Wilkes where they summarized, in detail, reports of its crystalline structure and various engineering properties associated with the amount and type of crystallinity [11]. Additionally, these authors investigated the effect of molecular

weight and branching units on PPS crystallization kinetics and modeled its kinetics both isothermally and non-isothermally using a single-mechanism model [17–18].

Several other investigators have also contributed significantly to understanding of PPS crystallization phenomena. Bludgell and Day focused on the effect of processing melt-residence time on the crystallization kinetics and reported an optimal processing window in order to avoid degradation [24]. Song *et al.* demonstrated through the use of seeding experiments that there is not a lack of nucleation sites for melt-crystallization and therefore nucleation is not rate-limiting in the crystallization process of PPS [20].

Quantitative dual-mechanism modeling of crystallization in unreinforced thermoplastics have been traditionally only been applied to aromatic ketones such as polyetheretherketone (PEEK) and polyetherketoneketone (PEKK) [27–31]. Additionally, dual-melting behavior in thermoplastics was reported by Lee and Porter in PEEK and was explained not on a dual-morphology basis, but on a melt/reorganization model due to the reheating of imperfect crystalline structures [32]. Chung and Cebe reported similar behavior in PPS, but after more extensive examination, they found that at a particular temperature, dependent on the inherent material kinetics, the melt/recrystallization behavior changed from a reorganization dominated regime to a morphologically dominated regime [21–23]. In order to explain this, these authors suggested a plausible molecular model in which they assert PPS crystallizes in a dual-mechanistic fashion where one mechanism is rapid and the other is 'normal'. Finally, Cheng *et al.* extensively studied the glass transition and melting behavior of PPS and noted many similarities between PPS and PEEK in their thermal and molecular transition behavior [1].

Several researchers have acknowledged the existence of a fast crystallization phenomena in PPS. Brady observed that perfectly amorphous PPS was not attainable through quench processing and Cheng *et al.* later reinforced these observations in greater molecular and kinetic detail [1, 4]. More recently, Huo *et al.* noted significant crystallinity in film processed PPS, which is quenched upon processing [33]. Chung and Cebe additionally reported an asymmetry of the melt crystallization and annealing crystallization (from "amorphous" material) half-times, which should theoretically be mirror images of one another about the peak crystallization temperature [21]. They note that the crystallization kinetics from the annealing side are faster than predicted, due to structure existing from the quenching process which act as nucleation sites for crystals to form faster.

However, even through these observations have been made, no quantitative model has yet been suggested that would account for both the isothermal and non-isothermal observations. Consequently, previous models have neglected the

early crystallization times or have assumed amorphous beginning materials when in fact they do not exist. In this present work, a quantitative model is presented that accounts for both the early and long time behavior for both isothermal and non-isothermal conditions which was developed from the generalized Velisaris and Seferis dual-mechanism crystallization methodology [28].

Modeling background

The crystallization kinetics of semi-crystalline thermoplastics have been addressed by many researchers using a variety of models [28, 34, 35]. Models based on Avrami kinetics are common, since it is a simple model that absorbs both nucleation and growth into a single expression [36–38]. Equation 1 shows the basic Avrami expression which assumes isothermal conditions and a single nucleation and growth type behavior [37].

$$\frac{X(t)}{X_\infty} = 1 - \exp[-k(T)t^n] \tag{1}$$

where:

$X(t)$ is the crystallinity at any time t
X_∞ is the maximum crystallinity at that temperature
$k(T)$ is the crystallization rate constant
T is the crystallization temperature
n is the 'Avrami' exponent

Thus, when isothermal crystallization data is plotted as lg t *vs.* lg{$-$ln[$X(t)$/$X(\infty)$]}, the resulting straight line will yield the Avrami exponent (slope) and rate constant (intercept). However, when Velisaris and Seferis plotted PEEK crystallization data in this way, two straight lines were observed instead of the usual one [28]. To model this unique behavior, they developed a dual-mechanism expression in which two Avrami crystallization mechanisms (F_i) act in parallel as suggested by analysis of the data, viz:

$$\frac{X(t)}{X_{(\infty)}} = w_1F_1 + w_2F_2 \tag{2}$$

where:

F_i is the i^{th} crystallization mechanism (Eq. 1)
w_i is a weighting function where $\Sigma w_i = 1$
and the rate constant $k(T)$ in each mechanism for Eq. (1) is defined by:

$$k_i(t) = C_{i1}T\exp\left\{-\left[\frac{C_{i2}}{(T - T_g + 51.6)} + \frac{C_{i3}}{T(T_m^\circ - T)^2}\right]\right\} \quad (3)$$

where:

T_m° is the equilibrium melt temperature ($\neq T_m$)
T_g is the glass transition temperature
C_{ij} are model constants [21]

The model constants C_{i2} and C_{i3} above are related to kinetic and thermodynamic expressions dealing with the chain transport activation energy and crystal surface free energies, respectively [28, 29, 35, 39]. It should also be noted here that the general expression $X(t)/X_{(\infty)}$ may refer to either volume or mass fraction crystallinities in the above equations, since their ratios are dimensionless. In this paper, all crystallinities, unless otherwise specified, are reported as volume fraction.

Velisaris and Seferis also developed non-isothermal expressions for each of the Avrami expressions in order to predict real processing behavior [28]. For this, they integrated the temperature dependence of the crystallization over the total time of cooling, viz:

$$F_i = 1 - \exp\left[-\int_0^t k_i(T)n_i t^{n_i - 1}dt\right] \quad (4)$$

and substituted into Eq. 1 to obtain the non-isothermal crystallization kinetics model.

Experimental

The PPS used in this study was provided by Phillips Petroleum. It was provided as thin films, opaque and yellowish in color with thicknesses of 7 and 10 μm. Transition temperatures for this material were determined by using a TA Instruments 910 Differential Scanning Calorimeter (DSC) interfaced with a TA Instruments 2000 computer/controller. The instrument was calibrated and operated in accordance with the operators manual. The glass transition temperature (T_g), which is rate dependent, was found to vary from 85–90°C and the peak melt temperature (T_m) (as distinguished from the equilibrium melt temperature, T_m°) was 280°C. All of these temperatures lie within a range of published values for PPS [1, 11]. The theoretical heat of fusion for 100% crystalline material (ΔH_f°) was reported by the manufacturer to be 104 J/g [40]. Since this value is not typical of other PPS materials, it may be assumed that the crystalline structures are slightly different, possibly allowing for the unique

crystallization behavior. Detailed crystal structure analysis via various radiation techniques as well as additional investigation as to this system's specific chemical structure and purity were not provided nor were they included as part of this study. A DSC thermogram of the as-received material heated at 10 deg·min^{-1} is shown in Fig. 1.

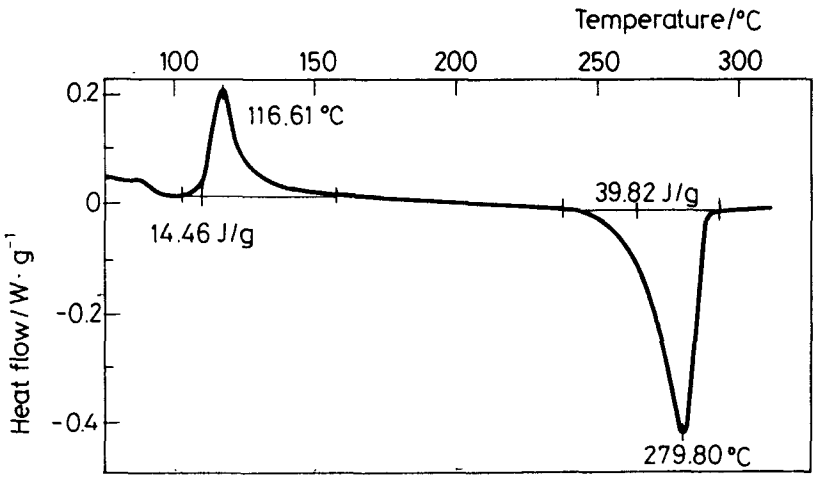

Fig. 1 DSC heating scan (10 deg·min^{-1}) of as-received PPS film

The crystallization kinetics of PPS were also investigated using the TA Instruments DSC system. Crystallization experiments were performed by first melting ~25 mg of PPS film at 340°C for five minutes in the DSC cell with a 40 ml·min^{-1}. Nitrogen flow to ensure complete melting of any crystalline phase in an inert atmosphere. Previous work has shown these conditions to be below the degradation threshold for PPS [24]. Isothermal experiments were then carried out by cooling the DSC cell as quickly as possible (~100 deg·min^{-1}) to the desired isothermal temperature through the use of an external cooling technique. Due to the mass of the DSC cell, a finite time was required for the sample to equilibrate at the crystallization temperature, but was consistently under one minute. The material was then held at the constant crystallization temperature for 120 minutes. After 120 minutes, the sample pan was removed from the DSC cell and immediately quenched in cold water. Non-isothermal experiments were carried out in a similar manner, except after the 5 minute hold at 340°C, the material was cooled, by using a TA Instruments Liquid Nitrogen Cooling Accessory (LNCA), to room temperature at the desired constant rate ranging from 1 to 40 deg·min^{-1}.

The resulting crystallinities of each sample were measured by DSC at a heating rate of 10 deg·min^{-1} to 340°C. The degree of crystallinity by mass is calculated using Eq.(5).

$$X_{mc} = \frac{(H_m - H_a)}{\Delta H_f^\circ} \tag{5}$$

where:

X_{mc} is the mass fraction crystallinity
H_m is the measured enthalpy of melting
H_a is the measured enthalpy of additional crystallization
ΔH_f° is the theoretical heat of fusion for the 100% crystalline phase

The volume fraction crystallinity may then be obtained through Eqs 6 and 7 if the necessary constants are known.

$$X_{vc} = \frac{\rho_m}{\rho_c} X_{mc} \tag{6}$$

$$\rho_m = \rho_c X_{vc} + (1 - X_{vc})\rho_a \tag{7}$$

where:

X_{mc} is the mass fraction crystallinity
X_{vc} is the volume fraction crystallinity
ρ_a is the density of t he amorphous phase
ρ_c is the density of the crystalline phase
ρ_m is the overall material density

The physical properties for PPS are shown in Table 1 [11, 40].

Table 1 PPS Material Properties [11, 40]

Property	Symbol	Value	Units
Engineering (Peak) melt temp.	T_m	280	°C
Glass transition temp.	T_g	85–90	°C
Density			
Crystalline PPS	ρ_c	1.42	g/cm^3
Amorphous PPS	ρ_a	1.11	g/cm^3
Heat of fusion (100% crystalline)	ΔH_f°	104	J/g

Rapid crystallization kinetics

During the isothermal crystallization analysis of PPS, the rapid crystallization phenomena was initially identified experimentally. Figures 1 and 2 illustrate the phenomena. Figure 2 is a rescan of a PPS sample cooled as rapidly as possible (~100 deg·min^{-1}) in the DSC to 240°C, which was the destination isothermal temperature in this example. Immediately after reaching 240°C, the sample was pulled out of the DSC cell and quenched in cold water in order to determine how much, if any, crystallinity had developed during the cooling stage of the experiment. The plot shows that there has already been significant crystallinity development before an isothermal environment was even reached since the cold-crystallization exotherm, upon reheating, is small. Therefore, any isothermal analysis at 240°C (or below) would give inaccurate results, since the majority of the crystallites had already formed non-isothermally.

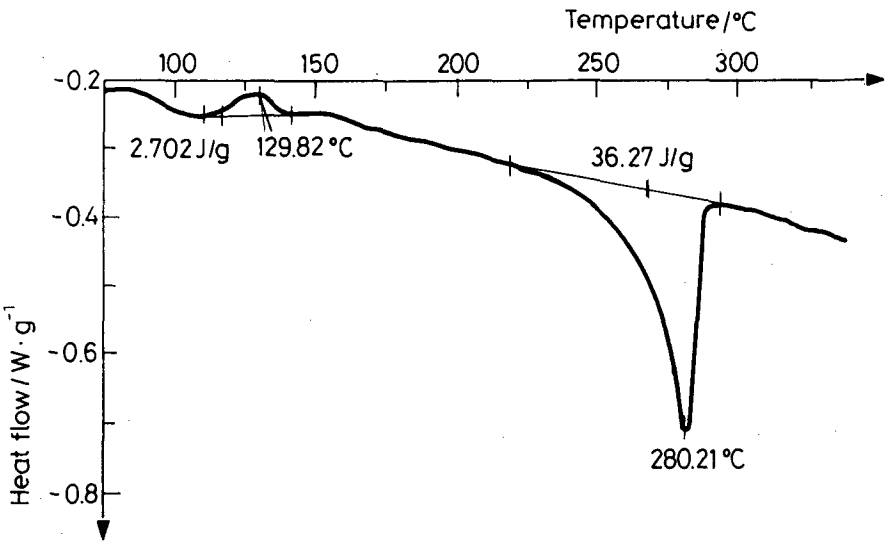

Fig. 2 DSC heating scan (10 deg·min^{-1}) of PPS quenched in water after cooling ~100 deg·min^{-1} to 240°C in the DSC from a 340°C melt

To illustrate the limiting behavior, Fig. 3 is a DSC scan of a PPS sample taken out of the DSC at 340°C after 5 minutes and immediately dropped in cold water. This should create an amorphous material. However, as the figure shows, the sample exhibited significant residual crystallinity. Based on calculations following Eq.(5), the sample had formed 8% by volume (10% crystallinity by mass) during the cooling. This reproducible result shows that the initial crystallization is difficult to control under normal processing conditions. A similar

phenomena was recently identified in thin-film processing, where significant crystallinity was observed microscopically after fast cooling [33].

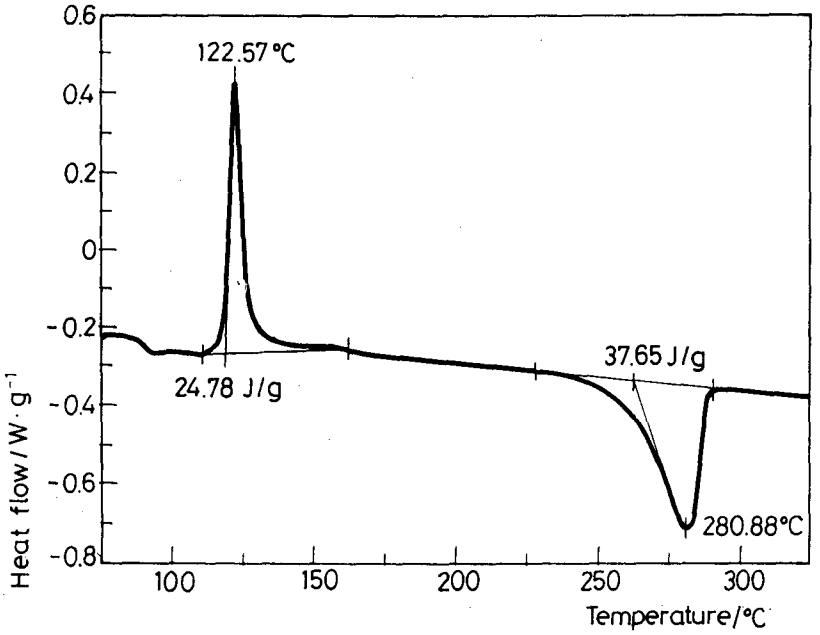

Fig. 3 DSC heating scan (10 deg·min^{-1}) of PPS quenched in water from a 340°C melt

In order to investigate the isothermal kinetics, crystallization temperatures would need to be chosen near the melt temperature where the crystallization proceeds slow enough, because the majority of crystallization was found to occur non-isothermally at all but the lowest levels of undercooling. Therefore, isothermal analysis of the unique phenomena was carried out at 260, 263 and 265°C.

To determine the Avrami exponent (Eq.(1)), the isothermal experimental crystallization data was lotted in a lg/lg form described earlier. The slope of the data yield the exponent, which is indicative of the type of nucleation and growth that occurred [35]. Figure 4 shows the lg/lg plot of the isothermal crystallization data at 265°C with the slope of the line suggesting an Avrami exponent of 2. Isothermal crystallization data at the other crystallization temperatures also had slopes of 2. Therefore, the crystallization model used this value as a constant.

The most intriguing aspect of the experimental portion of this work was that upon reheating the isothermal crystallized samples, there was always more energy liberated in the remelting of the developed crystals than could be ac-

counted for during the melt-crystallization and cold-crystallization peaks. In fact, this difference consistently corresponded to the same 8% crystallinity by volume discussed in Fig. 3. Thus, it was assumed that 8% (or 10% by mass) crystallinity always developed very rapidly and uncontrollably.

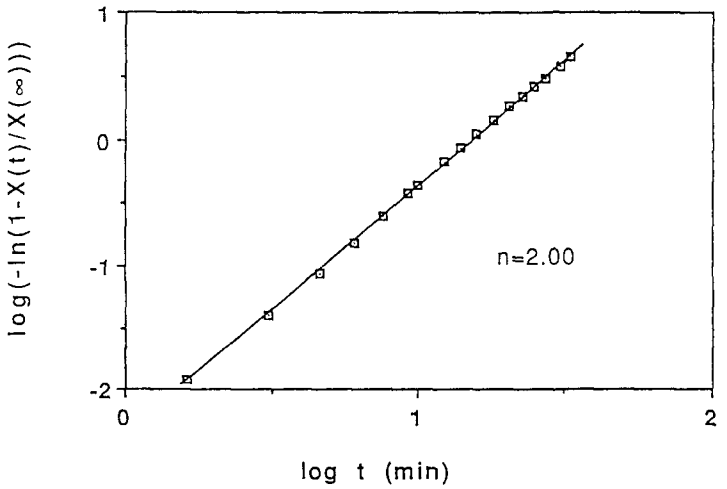

Fig. 4 Isothermal crystallization of PPS at 265°C

Crystallization modeling

To model this unique behavior, it was natural to approach this phenomena from a dual-mechanism standpoint. As discussed in the model background section, a previous dual-model (Eq. 2) utilized two independent Avrami mechanisms, each functionally dependent on time and temperature as shown in Eqs (1) and (3). This modeling methodology was then applied to PPS. Here, one mechanism occurs independent of time while the other mechanism followed a time/temperature dependent behavior which was modeled using Avrami kinetics, viz:

$$\frac{X(t)}{X_{(\infty)}} = w_1 F_1 + w_2 \tag{8}$$

where the weighing functions still sum to unity. It is this second mechanism, which follows Avrami kinetics that is classically identified as PPS crystallization kinetics. The importance of this model is its dual-mechanistic nature, necessary because of the identification and quantification of the very rapid initial crystallization kinetics. Additionally, the limiting case of this dual-mechanism model collapses into an equivalent description offered by Cheng and

Wunderlich for nucleation and grówth when a significant volume fraction of nuclei exists [41].

One other aspect of the crystallization modeling that needs to be addressed is the temperature dependence of the maximum volume fraction crystallinity ($X_{vc\infty}$). Recent modifications to the original Velisaris and Seferis model have applied the linear dependence of $X_{vc\infty}(T)$ to the cyrstallization model in order to use the same weighting functions for all non-isothermal conditions [42]. However, long time (2 h)othermal experiments at varying crystallization temperatures showed that the maximum crystallinity was found to have no dependence on temperature for PPS and therefore was constant. As illustrated in Fig. 5, the $X_{vc\infty}$ was determined to be 0.36 where the temperature indicated as 'T_r' is the temperature at which the recrystallization (or cold-crystallization) occurs upon reheating due to metastability or incomplete crystallization [35].

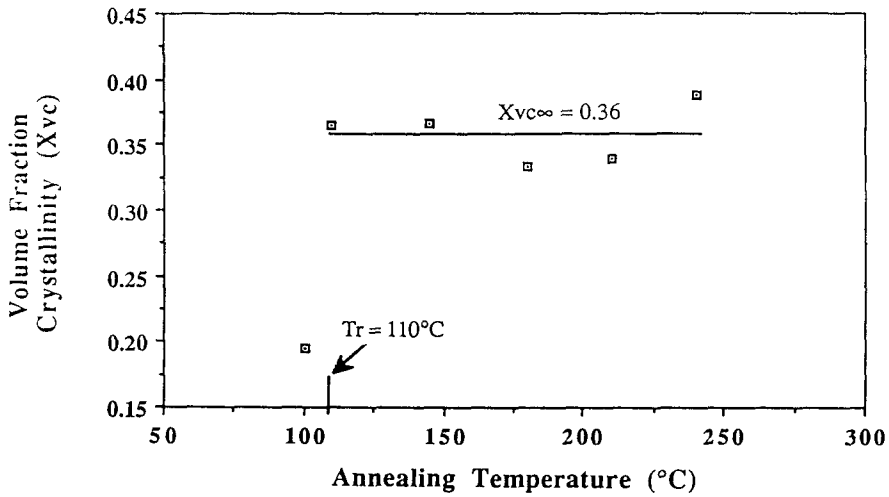

Fig. 5 Volume fraction crystallinity of PPS after 2 h of isothermal annealing

Additionally, since $X_{vc\infty}$ is a constant and the crystallinity exhibits a minimum of 8%, w_2 is fixed at a constant value of 0.22, which is equal to the ratio of minimum to maximum observed crystallinity by volume (0.08/0.36).

From the isothermal crystallization data, the crystallization constants C_{11}, C_{12} and C_{13} (in Eq. (3)) were experimentally determined and absorbed into $k_1(T)$. They are summarized in Tables 2 and 3 along with the other model parameter values. Figure 6 demonstrates how successfully the final isothermal model (Eq. (8)) predicts the isothermal crystallization data.

It should be explained here that while investigating this material a small range of T_g's for PPS was measured since the glass transition is a rate dependent phenomena. Since we are concerned with the cooling kinetics of crystallization

Table 2 PPS Isothermal crystallization rate constans $k_1(T)$

Temperature/°C	k/min^{-2}
260	1.03×10^{-1}
263	2.34×10^{-2}
265	1.25×10^{-2}

Table 3 Dual-mechanism modelconstants used for PPS crystallization modelling

Constant	Value
w_1	0.78
w_2	0.22
n_1	2.00
C_{11}/s^{-n}K^{-1}	1.6×10^6
C_{12}/K	5000
C_{13}/K^3	7.4×10^6
$T_m°$/K	573
T_m/K	558
T_g/K	363

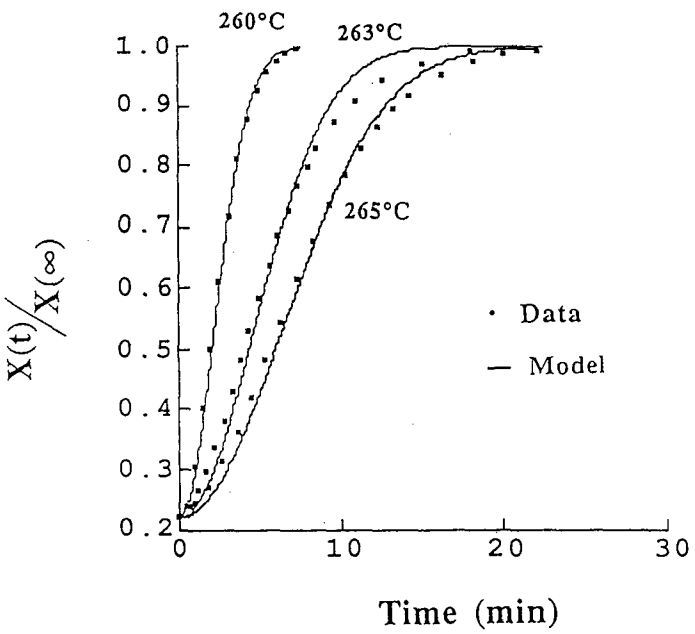

Fig. 6 Model predictions and experimental data for isothermal PPS crystallization

the T_g used in the kinetic modeling was the conservative or upper end value of 90°C (363 K). Additionally, the model development dictates the use of the equilibrium melting temperature. This value is typically significantly higher than the engineering or peak melt temperature as measured by DSC. Since the value of T_m° is determined experimentally and has been reported with uncertainty and variance, an approximate and conservative value of 300°C (573 K) was chosen for the model [1].

The unique thrust of this work lies in the non-isothermal extension from the isothermal model. The non-isothermal model follows the same development as the isothermal model. Since the initial mechanism is not a function of time or temperature, it will be unchanged in the non-isothermal model. Thus, the non-isothermal model takes on the same form as the isothermal model (Eq. 8) except the Avrami expression must be modified for non-isothermal conditions as shown in Eq. (4), viz.:

$$\frac{X(t)}{X_{(\infty)}} = w_1\left\{1 - \exp\left[-\int_0^t k_1(T(t))n_1 t^{n_1-1}dt\right]\right\} + w_2 \tag{9}$$

where, again the weight fractions w_1 and w_2 sum to 1. It is important to note that for the non-isothermal condition, a constant cooling rate (β) is assumed.

$$\beta = -\frac{dT}{dt} \tag{10}$$

Equating time to temperature in Eq. (9) by Eq. (10) requires the limits of integration to be changed from 0 to t, to T_m (285°C) to T_g (90°C). Here the high end onset melt temperature of 285°C (558 K) was used in the limits of the integration, not the peak melt temperature, since the cyrstallization occurs by cooling from the melt. Substituting Eq. (10) into (9) results in the final form of the non-isothermal model, viz:

$$\frac{X(t,T)}{X_{(\infty)}} = w_1\left\{1 - \exp\left[\left(\frac{-1}{\beta}\right)^{n_1}\int_{T_m}^{T_g} k_1(T)n_1 T^{n_1-1}dT\right]\right\} + w_2 \tag{11}$$

Most importantly, all of the model parameter values are the same for both isothermal and non-isothermal processes. Therefore, the model parameters do not have to be altered accommodate different processing conditions. This is significant because PPS crystallization kinetics have never been previously described utilizing this dual-approach for both isothermal and non-isothermal

conditions. Finally, the weighting functions are not expected to change with the addition of a fiber reinforcement phase for use in polymeric matrix composites.

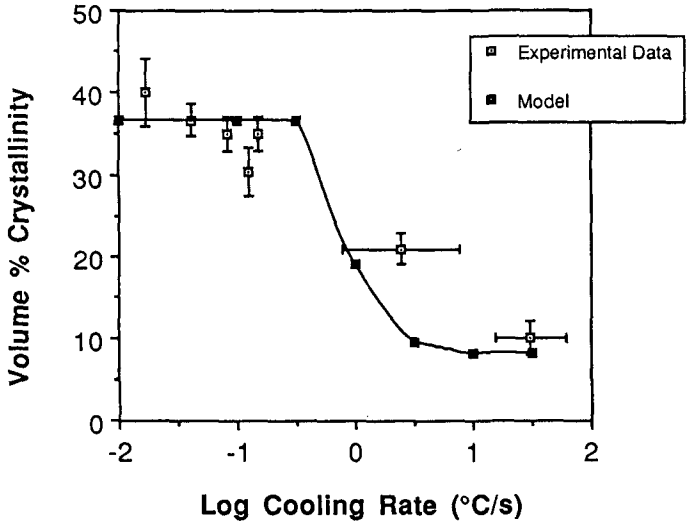

Fig. 7 Dual model predictions (Eq. (11)) and data for PPS volume fraction crystallinity as a function of cooling rate

Figure 7 shows non-isothermal model predictions along with the experimental data. Error bars have been included to illustrate the variability of the cooling rate using external cooling techniques while the slower cooling rates are precisely controlled in the DSC. At first, the data appears to lie along a straight line, however, since the minimum crystallinity is 8%, data points obtained at extremely fast cooling rates would still lie at 8%. Thus, a straight line fit would not model this base plateau and it would errantly predict the material reaching 0% crystallinity through extrapolation. Additionally, similar upper and lower plateau behavior was observed for PEEK crystallization in which a dual model was required to model a complex system [28]. This principle of applying a practical engineering methodology played a key role in the modeling in order to fully and accurately represent the observed behavior. Therefore, the crystallization model represents a useful and practical representation of the crystallization behavior of PPS.

In order to quantify the non-isothermal model sensitivity to the constants C_{11}, C_{12} and C_{13}, calculations were made by varying the parameter values by ±10%. Figures 8a–c illustrate the non-isothermal model sensitivity on the constants by plotting ±10% variations of C_{11}, C_{12} and C_{13} respectively.

Obviously, the model is most sensitive to C_{12}. Since C_{12} is related to the chain transport activation energy, which is a kinetic *vs.* a thermodynamic phe-

nomena, the model suggests that PPS crystallization is rate limited by the ability of chains to migrate to the growing crystals.

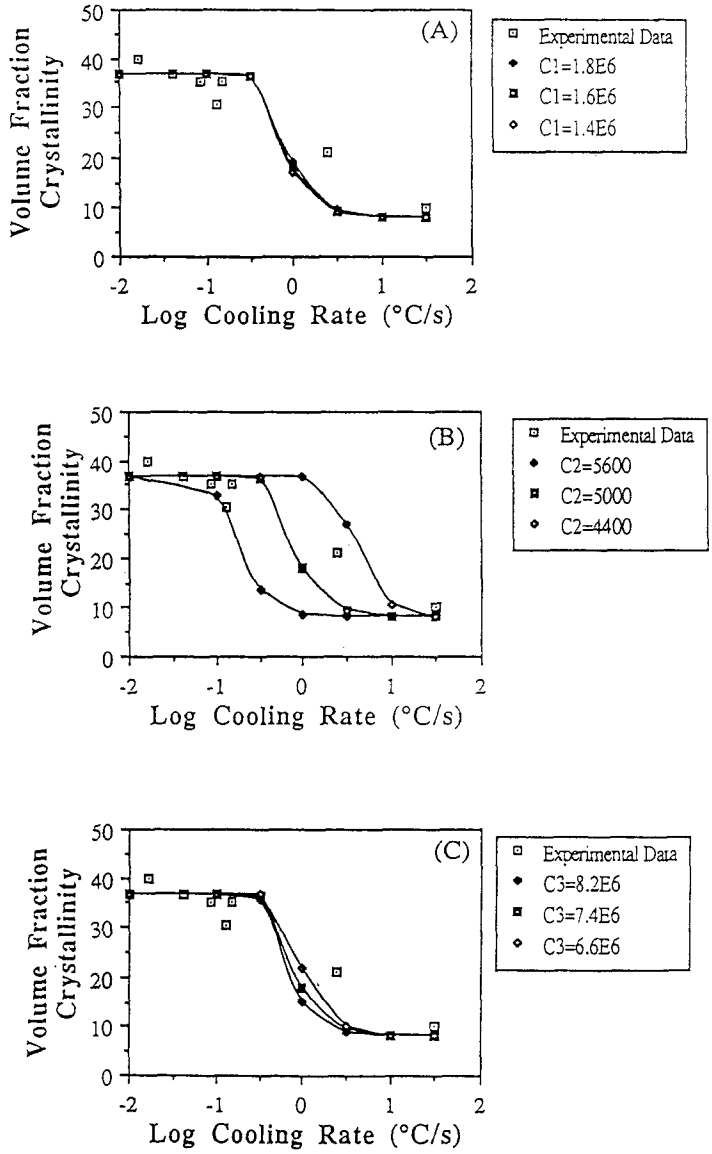

Fig. 8 Non-isothermal model sensitivity to ±10% variations of model constants C_{11}, C_{12} and C_{13}

Finally, Eqs (2) and (8) illustrate how this model is really a special case of the more general dual-mechanism model originally proposed by Velisaris and Se-

feris [28]. Here, $k_1(T)$ and F_1 take on identifical functionality as shown in Eqs (1) and (3), whereas F_2 from the general dual-mechanism model (Eq. (2)) is not a function of time or temperature. As a result of this Velisaris-Seferis model extension to predict PPS kinetics, the versatility of the model is brought to light. It illustrates the flexibility of the original dual-mechanism model as a general case. Therefore, with tailored modifications, the general Velisaris-Seferis model may be used to describe the crystallization kinetics of additional material systems other than PEEK.

Conclusions

The model presented in this work quantitatively describes PPS isothermal and non-isothermal crystallization kinetics in a dual-mechanistic fashion for the first time. The modeling methodology was based on the previous work of Velisaris and Seferis where it provided a general case of dual-mechanism crystallization modeling. This work identified the fast initial crystallization kinetics of melt-crystallized PPS followed by the normally identified Avrami crystallization kinetics. It is this fast mechanism that results in a minimum of 8% crystallinity by volume under all processing conditions. The model also predicted that PPS crystallization kinetics are rate limited by the ability of chains to migrate to the growing crystals.

The practical application of this work is that the rapid nature of the crystallization process resulting in the minimum crystallinity level for this material may influence the final end-use (i.e. mechanical and chemical) properties of the material, which must be accounted for in actual process engineering [12–16]. Finally, this work emphasizes the general nature of the dual-mechanism modeling methodology presented by Velisaris and Seferis to other dual-behavior type material systems.

* * *

The authors would like to express their appreciation to C. N. Velisaris of the Polymeric Composites Laboratory for helpful technical discussions concerning this work. Financial assistance for this work was provided by the Boeing Company and Phillips Petroleum through project support to the Polymeric Composites Laboratory of the University of Washington.

References

1 S. Z. D. Cheng, Z. Q. Wu and B. Wunderlich, Macromol., 20 (1987) 2802.
2 S. Z. D. Cheng, R. Pan, M.-Y. Cao, and B. Wunderlich, Makromol. Chem., 189 (1988) 1579.
3 A. J. Lovinger, F. J. Padden, Jr., and D. D. Davis, Polymer, 29 (1988) 229.
4 D. G. Brady, J. Appl. Polym. Sci. Pt. B, 20 (1976) 2541.

5 P. Grenvesse, Bull. Soc. Chim. France, 17 (1897) 599.
6 J. T. Edmonds and H. W. Hill, Jr., U. S. Patent 3, 354, 129 (Nov. 1967).
7 S. Tsunawaki and C. C. Price, J. Polym. Sci., 2A (1964) 1511.
8 B. J. Tabor, E. P. Magree, and J. Boon, Europ. Polym. J., 7 (1971) 1127.
9 H. W. Hill, Jr. and D. G. Brady, Polym. Eng. Sci., 16 (1976) 832.
10 J. N. Short and H. W. Hill, Jr., Chem. Tech., 2 (1972) 481.
11 L. C. Lopez and G. L. Wilkes, Rev. Macromol. Chem. Phys., C29 (1989) 83.
12 I. M. Ward, 'Mechanical Properties of Solid Polymers', Wiley & Sons, New York 1983.
13 P. C. Powell, 'Engineering with Polymers', Chapman and Hall Ltd., London 1983.
14 E. J. Stober, J. C. Seferis and J. D. Keenan, Polymer, 25 (1984) 1854.
15 W. E. Lawrence, J.-A. E. Manson and J. C. Seferis, Composites, 21 (1990) 475.
16 W. E. Lawrence, J. C. Seferis and J. W. Gillespie, Jr., Polym. Comp., 13 (1992) 86.
17 L. C. Lopez and G. L. Wilkes, Polymer, 29 (1988) 106.
18 L. C. Lopez and G. L. Wilkes, Polymer, 30 (1989) 882.
19 L. C. Lopez, G. L. Wilkes and J. F. Geibel, Polymer, 30 (1989) 147.
20 S. S. Song, J. L. White and M. Cakmak, Polym. Eng. Sci., 30 (1990) 944.
21 J. S. Chung and P. Cebe, J. Polym. Sci., 30 (1992) 163.
22 J. S. Chung and P. Cebe, Polymer, 33 (1992) 2312.
23 J. S. Chung and P. Cebe, Polymer, 33 (1992) 2325.
24 D. Budgell and M. Day, Polym. Eng. Sci., 31 (1991) 1271.
25 W. J. Lee, B. K. Fukai, J. C. Seferis and I. Y. Chang, Composites, 19 (1988) 473.
26 W. E. Lawrence, Ph. D. Dissertation, Dept. of Chem. Eng., Univ. of Washington (1992).
27 J. A. Ferrara and J. C. Seferis, Proc. 5th Europ. Conf. Comp. Mtls., (1992) 853.
28 C. N. Velisaris and J. C. Seferis, Polym. Eng. Sci., 26 (1986) 1574.
29 P. Cebe, Polym. Eng. Sci., 28 (1988) 1192.
30 J. A. Ferrara, J. C. Seferis and G. Vassilatos, 23rd SAMPET Tech. Conf., (1991) 1137.
31 B. S. Hsiao, I. Y. Chang and B. B. Sauer, Polymer, 32 (1991) 2799.
32 Y. Lee and R. S. Porter, Polym. Eng. and Sci., 26 (1986) 9.
33 P. P. Huo, J. S. Chung and P. Cebe, Polym. Comp., 13 (1992) 346.
34 A. Wasiak, Chemtracts-Macromol. Chem., 2 (1991) 211.
35 B. Wunderlich, 'Macromolecular Physics', Vol. 2, Academic Press, New York 1976.
36 M. Avrami, J. Chem. Phys., 7 (1939) 1103.
37 M. Avrami, J. Chem. Phys., 8 (1940) 212.
38 M. Avrami, J. Chem. Phys., 9 (1941) 177.
39 J. T. Hoffman, G. T. Davis and J. I. Lauritzen, 'Treatise on Solid State Chemistry', Vol. 3. B. N. Hannay, Ed., Plenum Press, New York 1976.
40 Data supplied by R. L. Hagenson, Phillips Petroleum, (February 1990).
41 S. Z. D. Cheng and B. Wunderlich, Macromol., 21 (1988) 3327.
42 C. N. Velisaris and J. C. Seferis, in preparation (1994).

Zusammenfassung — Die Untersuchungen zeigen, daß Polyphenylensulfid (PPS) auf eine ungewöhnliche doppelmechanistische Art kristallisiert, wobei 8 Vol% der Substanz unmittelbar kristallisieren, während der verbleibende Teil der Substanz auf eine zeitabhängige Art und Weise kristallisiert. Diese schnelle Schmelz-Kristallisationskinetik wurde unter Anwendung eines Doppelmechanismusmodelles modelliert, welches auf der zuerst von Velisaris und Seferis bei der Kristallisation von Polyetheretherketonen (PEEK) beobachteten Methodologie basiert. Anschließend wird das Kristallisationsmodell in einem weiten Intervall von Kühlgeschwindigkeiten

und unter gleichen Modellparametern zur genauen Voraussage von sowohl isothermem als auch – erstmalig – nichtisothermem Kristallisationsverhalten verwendet. Vorliegende Arbeit kennzeichnet und modelliert die Kinetik der schnellen Anfangskristallisation von PPS. Zusätzlich wurde die Flexibilität des Doppelmechanismusmodelles von Velisaris und Seferis an PPS dadurch bestätigt, indem gezeigt wurde, daß es sich um einen Spezialfall der allgemeinen Methodologie der Doppelkristallisationskinetik handelt.